Application of Physiologically Based Pharmacokinetic Modeling in Understanding Bosutinib Drug-Drug Interactions: Importance of Intestinal P-Glycoprotein[S]

Shinji Yamazaki, Cho-Ming Loi, Emi Kimoto, Chester Costales, and Manthena V. Varma

Pharmacokinetics, Dynamics and Metabolism, Pfizer Worldwide Research & Development, San Diego, California (S.Y., C.-M.L.) and Groton, Connecticut (E.K., C.C., M.V.V.)

ABSTRACT

Bosutinib is an orally available Src/Abl tyrosine kinase inhibitor indicated for the treatment of patients with Ph+ chronic myelogenous leukemia at a clinically recommended dose of 500 mg once daily. Clinical results indicated that increases in bosutinib oral exposures were supraproportional at the lower doses (50–200 mg) and approximately dose-proportional at the higher doses (200–600 mg). Bosutinib is a substrate of CYP3A4 and P-glycoprotein and exhibits pH-dependent solubility with moderate intestinal permeability. These findings led us to investigate the factors influencing the underlying pharmacokinetic mechanisms of bosutinib with physiologically based pharmacokinetic (PBPK) models. Our primary objectives were to: 1) refine the previously developed bosutinib PBPK model on the basis of the latest oral bioavailability data and 2) verify the refined PBPK model with P-glycoprotein kinetics on the basis of the bosutinib drug-drug interaction (DDI) results with ketoconazole and rifampin. Additionally, the verified PBPK model was applied to predict bosutinib DDIs with dual CYP3A/P-glycoprotein inhibitors. The results indicated that 1) the refined PBPK model adequately described the observed plasma concentration-time profiles of bosutinib and 2) the verified PBPK model reasonably predicted the effects of ketoconazole and rifampin on bosutinib exposures by accounting for intestinal P-glycoprotein inhibition/induction. These results suggested that bosutinib DDI mechanism could involve not only CYP3A4-mediated metabolism but also P-glycoprotein-mediated efflux on absorption. In summary, P-glycoprotein kinetics could constitute an element in the PBPK models critical to understanding the pharmacokinetic mechanism of dual CYP3A/P-glycoprotein substrates, such as bosutinib, that exhibit nonlinear pharmacokinetics owing largely to a saturation of intestinal P-glycoprotein-mediated efflux.

Introduction

For predicting and understanding pharmacokinetics, drug-drug interactions (DDIs), drug-disease interactions, and pediatric/geriatric therapies of new molecular entities (NMEs), mechanistic modeling and simulation approaches are being applied increasingly to all phases of drug discovery and development, as well as to regulatory decisions on labeling languages (Rowland et al., 2011; Huang and Rowland, 2012; Wagner et al., 2015, 2016; Shebley et al., 2018). Among the modeling and simulation approaches, a physiologically based pharmacokinetic (PBPK) model is a powerful tool to quantitatively predict DDIs on the basis of drug-dependent physicochemical and pharmacokinetic parameters along with drug-independent physiological systems parameters (Lave et al., 2007; Nestorov, 2007; Rowland et al., 2011; Jones and Rowland-Yeo, 2013; Jones et al., 2015). Recently, the US Food and Drug Administration (FDA), the European Medicines Agency (EMA), and the Japanese Pharmaceuticals and Medical Devices Agency

(PMDA) have issued DDI guidances, which highlight the use of integrated mechanistic approaches, including PBPK models: (http://www.ema.europa.eu/docs/en_GB/document_library/Scientific_guideline/2012/07/WC500129606.pdf; http://www.nihs.go.jp/mss/T140710-jimu.pdf; https://www.fda.gov/downloads/drugs/guidancecomplianceregulatoryinformation/guidances/ucm292362.pdf; https://www.fda.gov/downloads/Drugs/GuidanceComplianceRegulatoryInformation/Guidances/UCM581965.pdf). Accordingly, there has been a growing emphasis in developing PBPK models to assess potential DDI risks of NMEs in a drug discovery and development setting.

Bosutinib (Bosulif), an orally available Src/Abl tyrosine kinase inhibitor, has been approved globally for the treatment of adult patients with chronic, accelerated, or blast phase Ph+ chronic myelogenous leukemia with resistance or intolerance to prior therapy (http://www.accessdata.fda.gov/drugsatfda_docs/label/2016/203341s006lbl.pdf). Clinically recommended dose of bosutinib is 500 mg once daily under fed conditions. Bosutinib is a substrate of CYP3A4 and P-glycoprotein (P-gp) and exhibits pH-dependent aqueous solubility over the pH range of 1–8 with moderate in vitro passive permeability (http://www.accessdata.fda.gov/drugsatfda_docs/nda/2012/203341Orig1s000ClinPharmR.pdf). In phase I

ABBREVIATIONS: ADAM, advanced dissolution, absorption, and metabolism; AUC, area under the plasma concentration-time curve; AUCR, AUC ratio; CL_{int}, intrinsic clearance; C_{max}, maximum plasma concentration; $C_{max}R$, C_{max} ratio; DDI, drug-drug interaction; F_a, fraction of the dose absorbed from gastrointestinal tract; F_g, fraction of the dose that escapes intestinal first-pass metabolism; F_h, fraction of the dose that escapes hepatic first-pass metabolism; f_u, unbound fraction; NME, new molecular entity; PBPK, physiologically-based pharmacokinetic(s); P-gp, P-glycoprotein; P/O, predicted-to-observed pharmacokinetic parameters; SAO, sensitivity analysis and optimization; SF, scaling factor; t_{max}, time to reach maximum plasma concentration; V_{ss}, volume of distribution at steady-state.

studies, increases in bosutinib exposures, estimated as maximum plasma concentration (C_{max}) and area under the plasma concentration-time curve (AUC), were supraproportional at doses of 50–200 mg and approximately dose-proportional at doses of 200–600 mg (http://www.accessdata.fda.gov/drugsatfda_docs/nda/2012/203341Orig1s000ClinPharmR.pdf). In contrast, bosutinib terminal half-lives were comparable between these doses (i.e., 13–22 hours). Since bosutinib is a substrate of P-gp, the nonlinear-to-linear pharmacokinetic profiles from lower to higher doses could be considered owing mainly to a saturation of intestinal P-gp-mediated efflux on absorption, resulting in dose-dependent increases in a fraction of the dose absorbed from the gastrointestinal tract (F_a). These findings led us to investigate the factors influencing the underlying pharmacokinetic mechanisms with PBPK models.

Bosutinib is predominantly metabolized by CYP3A4 as the primary clearance mechanism in humans with minimal urinary excretion (<2% of the administered dose) (http://www.accessdata.fda.gov/drugsatfda_docs/nda/2012/203341Orig1s000ClinPharmR.pdf; Syed et al., 2014). For the potential DDI risk assessment as the CYP3A4 substrate, bosutinib single-dose DDI studies were conducted in healthy volunteers with coadministration of a strong CYP3A inhibitor, ketoconazole (400 mg once daily), and a strong CYP3A inducer, rifampin (600 mg once daily) (Abbas et al., 2011, 2012, 2015). Bosutinib exposures estimated as C_{max} and AUC increased by up to 9-fold when coadministered with ketoconazole, and decreased by ~90% when coadministered with rifampin. Accordingly, the US prescribing information advises avoidance of concurrent use of bosutinib with strong or moderate CYP3A inhibitors and inducers (http://www.accessdata.fda.gov/drugsatfda_docs/label/2016/203341s006lbl.pdf). A postmarketing requirement by FDA was issued to evaluate the effect of moderate CYP3A4 inhibitors on bosutinib exposures to identify an appropriate dose when used concomitantly with moderate CYP3A inhibitors (http://www.accessdata.fda.gov/drugsatfda_docs/nda/2012/203341Orig1s000ClinPharmR.pdf). Accordingly, we developed bosutinib PBPK models to predict clinical DDIs with less potent CYP3A inhibitors (Ono et al., 2017). The model-predicted results (2- to 4-fold) with several moderate CYP3A inhibitors were consistent with the observed results (~2-fold) with a moderate CYP3A inhibitor, aprepitant (125 mg) (Hsyu et al., 2017). We also applied the PBPK models to predict changes in bosutinib steady-state exposures in patients with renal and hepatic impairment (Ono et al., 2017).

It has become a common practice to verify PBPK models of NMEs and refine the models, if necessary, when new datasets are available during drug development. Recently, an absolute oral bioavailability (F_{oral}) study of bosutinib was conducted in healthy subjects following an intravenous 1-hour infusion of 120 mg and an oral dose of 500 mg (Hsyu et al., 2018). However, the predicted bosutinib exposures by the previously developed PBPK model could not sufficiently match the results observed in the F_{oral} study, indicating that a further refinement of bosutinib PBPK model was required to adequately describe clinically observed results. Accordingly, we refined the previously developed bosutinib PBPK model on the basis of the latest F_{oral} data and verified the refined PBPK model with P-glycoprotein kinetics on the basis of single-dose bosutinib DDI results. In addition, the verified PBPK model was applied to predict bosutinib DDIs under clinical scenarios that have not been tested. In these modeling processes, we focused on 1) understanding the contribution of intestinal P-gp-mediated efflux to bosutinib pharmacokinetics and 2) quantitatively rationalizing bosutinib DDI mechanism by ketoconazole and rifampin.

Materials and Methods

Bosutinib Pharmacokinetic Studies in the Clinic

Detailed information from bosutinib clinical studies, such as a single-dose F_{oral} study in healthy volunteers and single-dose DDI studies with ketoconazole and rifampin in healthy volunteers, have been reported previously (Abbas et al., 2010, 2011, 2012; Hsyu et al., 2018) Additional information about bosutinib pharmacokinetics is also available in the FDA website (http://www.accessdata.fda.gov/drugsatfda_docs/nda/2012/203341Orig1s000ClinPharmR.pdf). Briefly, the F_{oral} study of bosutinib was conducted as a two-way crossover design in healthy male subjects ($n = 13$–14) under fed conditions (Hsyu et al., 2018). A single dose of bosutinib was administered to subjects either intravenously (120 mg in a 1-hour infusion) or orally (500 mg; 100-mg tablet × 5), and plasma concentrations of bosutinib were determined up to 7 days postdose. For the bosutinib DDI assessment, three single-dose studies were conducted in healthy male and female subjects with multiple-dose coadministration of ketoconazole (two studies at bosutinib doses of 100 and 500 mg) and rifampin (one study at bosutinib dose of 500 mg) (Abbas et al., 2011, 2012, 2015). In the bosutinib 100-mg DDI study with ketoconazole, each subject ($n = 24$) received a single oral dose of 100 mg bosutinib (day 1) in a fasted state either alone (control group) or with 5-day repeated oral doses of 400 mg ketoconazole once daily on days 0–4 (treatment group). In the bosutinib 500-mg DDI study with ketoconazole, each subject ($n = 54$–56) received a single oral dose of 500 mg bosutinib (day 1) in a fed state either alone (control group) or with 4-day repeated oral doses of 400 mg ketoconazole once daily on days 0–4 (treatment group). In the bosutinib 500-mg DDI study with rifampin, each subject ($n = 22$–24) received a single oral dose of 500 mg bosutinib (days 1 and 14) in a fed state with 10-day repeated oral doses of 600 mg rifampin once daily (days 8–17). Plasma concentrations of bosutinib in all subjects were determined up to 72 or 96 hours postdose in these DDI studies.

Bosutinib Input Parameters in the PBPK Model

A commercially available dynamic PBPK model, Simcyp population-based simulator (version 17.1; Simcyp Ltd., Sheffield, United Kingdom), was used in the present study (Jamei et al., 2009a). First, the previously developed PBPK model was refined on the basis of the latest F_{oral} results as mentioned before. The main differences in bosutinib input parameters between the previous and present PBPK models were hepatic microsomal intrinsic clearance (CL_{int}) and steady-state volume of distribution (V_{ss}). In addition, we used the advanced dissolution, absorption, and metabolism (ADAM) model implemented in Simcyp to incorporate intestinal P-gp kinetic parameters into the present PBPK model. In the ADAM model, the gastrointestinal tract is divided into nine different regions, namely stomach, duodenum, jejunum I and II, ileum I, II, III and IV, and colon, as subcompartments. Physicochemical and pharmacokinetic parameters of bosutinib used for the present PBPK models are summarized in Table 1.

Input Parameters for CL. The value of CL_{int} (560 μl/min per milligram protein) in the present model was back-calculated from an intravenous plasma clearance (~62 l/h) estimated in the F_{oral} study using a retrograde model implemented in Simcyp, whereas that (300 μl/min per milligram protein) in the previous model was estimated from a clinically observed oral clearance (~200 l/h) (Ono et al., 2017). Thus, a fraction of the dose that escapes hepatic first-pass metabolism (F_h) was estimated to be approximately ~0.5 on the basis of the intravenous blood clearance (~0.74 l/h per kilogram) given that the primary clearance mechanism was CYP3A4-mediated hepatic metabolism. Since a fraction of the dose metabolized by CYP3A4 ($f_{m,CYP3A4}$) was estimated as near-unity on the basis of the in vitro cytochrome P450 phenotyping and the human mass-balance study, the back-calculated CL_{int} values were subsequently assigned as CYP3A4-mediated metabolic CL_{int} in human liver microsomes in PBPK models. The input value of CL_{int} in human liver microsomes was scaled to CYP3A4-mediated intestinal clearance by accounting for CYP3A4 abundance in liver and intestine. Bosutinib renal clearance (CL_{renal}) was set at 1.2 l/h (~2% of systemic clearance) on the basis of the mass-balance results.

Input Parameters for V_{ss}. The V_{ss} input (28 l/kg) in the present PBPK model was a clinical estimate in the F_{oral} study, whereas that in the previous model (15 l/kg) was a mean value of the predicted human V_{ss} from single-species scaling for unbound V_{ss} values from mice, rats, and dogs (12–21 l/kg) with an exponent of unity (Ono et al., 2017). The predicted V_{ss} value by the tissue composition-based mathematical model implemented in Simcyp (as prediction method 2) was 7.5 l/kg (Rodgers et al., 2005); therefore, K_p scalars of 2.0 and 3.7 were used to set V_{ss} inputs of 15 and 28 l/kg, respectively.

Absorption Models. A fraction of the dose absorbed (F_a) was estimated at approximately 0.7 in a single-dose human mass-balance study with [^{14}C]bosutinib at a dose of 500 mg since the recovery of bosutinib (as the parent drug) in feces was 30% of the administered dose and the fecal recovery of bosutinib was unlikely

TABLE 1

Physicochemical and pharmacokinetic parameters of bosutinib used for PBPK models

Parameter (U)	Value	Source
Molecular weight	530	Calculated
LogP	3.1	Measured
pK_a (monobase)	7.9	Measured
$f_{u,plasma}$	0.063	Measured in vitro
B/P	1.2	Measured in vitro
F_a[a]	0.3–0.7	Mass-balance study results
k_a (h^{-1})[a]	0.13	Clinical study results
Lag time (h)[a]	1	Clinical study results
Solubility (mg/ml)	0.02–11 (at pH 1–8)	Measured in vitro
$P_{eff,man}$ $(10^{-4}$ cm/s)	1.8	Calculated from in vitro data
Q_{gut} (l/h)[a]	8.7	Calculated by Simcyp
$f_{u,gut}$	0.063	Predicted by sensitivity analysis
V_{ss} (l/kg)	28	Clinical study results
K_p scalar	3.7	Adjusted to predict the observed V_{ss} value
$CL_{int,CYP3A4}$ (μl/min per milligram protein)[b]	560	Back-calculated in Simcyp
CL_{renal} (l/h)	1.2	Clinical study results
P-gp K_m (μM)[c]	0.38	Measured in Caco-2 cells
P-gp J_{max} (pmol/min)[c]	15	Measured in Caco-2 cells
P-gp J_{max} SF[c]	1–25	Optimized to recover the observed results

[a]Input parameters used for PBPK-F_a models.
[b]Human liver microsomal CL_{int} back-calculated from the clinically observed clearance (~62 l/h) using a retrograde model.
[c]Intestinal P-pg parameters used for PBPK-ADAM models.

confounded by biliary excretion of the unchanged drug and/or reversible metabolites on the basis of the metabolic profiling results in the clinical studies, including a mass-balance study (Abbas et al., 2010; http://www.accessdata.fda.gov/drugsatfda_docs/nda/2012/203341Orig1s000ClinPharmR.pdf; Ono et al., 2017). Therefore, bosutinib F_a was set at 0.7 at a dose of 500 mg in the PBPK models with the first-order absorption rate constants (henceforth referred to as PBPK-F_a models). Furthermore, the ADAM model was used to incorporate intestinal P-gp kinetics into bosutinib absorption (henceforth referred to as PBPK-ADAM models). It may be worth noting that P-gp kinetics can be incorporated only into the PBPK-ADAM models in Simcyp (Jamei et al., 2009b). The regional distribution of P-gp abundance along with cytochrome 450 enzymes in intestine and its variability derived from meta-analysis of reported protein and mRNA values are incorporated into the population library of Simcyp (e.g., a virtual population of healthy volunteers). To predict bosutinib F_a, the ADAM models integrate the physicochemical and biopharmaceutical properties of bosutinib such as pH-dependent solubility (11, 9.4, 6.1, 2.7, 0.02, and 0.053 mg/ml at pH 1, 2, 4.5, 5, 6.8, and 8, respectively) and the intestinal effective permeability (1.8×10^{-4} cm/s) calculated from in vitro passive permeability (~7×10^{-6} cm/s) in low-efflux Madin-Darby canine kidney cells (Di et al., 2011; http://www.accessdata.fda.gov/drugsatfda_docs/nda/2012/203341Orig1s000ClinPharmR.pdf). In addition, the disintegration profile was defined in the ADAM models by the first-order kinetics with 100% maximal disintegration, a disintegration constant of 0.01 hour^{-1} and a lag time of 0.25 hours. Bosutinib in vitro P-gp kinetics were determined in the Caco-2 permeability study at the concentrations of 1–100 μM (http://www.accessdata.fda.gov/drugsatfda_docs/nda/2012/203341Orig1s000ClinPharmR.pdf). The estimated K_m (concentration required to achieve half of the maximal transport rate) and J_{max} (maximal transport rate) were 3.8 μM and 15 pmol/min, respectively, on the basis of the kinetic model (Tachibana et al., 2010). This model assumes steady-state condition to calculate kinetic parameters; therefore, the obtained K_m value was corrected for in vitro non-specific binding (~0.1) as an extracellular nonspecific binding, resulting in the unbound K_m of 0.38 μM as an input parameter. These calculations were performed with GraphPad Prism 6 (GraphPad Software Inc., San Diego, CA). In the PBPK-ADAM models, an in vitro-to-in vivo scaling factor (SF) for P-gp J_{max} was optimized to adequately recover the observed results, whereas K_m was assumed to be intrinsic and was fixed.

PBPK Simulation by Simcyp

To understand bosutinib pharmacokinetics, our modeling and simulation approaches are practically categorized into three main tiers: 1) model refinement on the basis of the latest F_{oral} data, 2) model verification on the basis of the single-dose bosutinib DDI results, and 3) model application to predict bosutinib DDIs under possible scenarios that have not been tested clinically. In these processes,

sensitivity analysis and optimization (SAO) for the model input parameters such as unbound fraction (f_u) in gut ($f_{u,gut}$) and SFs for P-gp J_{max} were performed as the model refinement and verification. Outlines of the PBPK modeling and simulation are summarized in Table 2 along with key parameters explored.

Simulation Outlines. Simulation of all clinical trials in Simcyp was performed with a virtual population of healthy volunteers in six trials of six subjects (total 36 subjects), each aged 20–50 years with a female/male ratio of 0.5, whose CYP3A4 degradation rate constant (k_{deg}) was 0.0193 hour^{-1} in liver and 0.03 hour^{-1} in intestine. The output sampling interval in Simcyp simulation tool box was set to 0.2 hours in all simulations. In the PBPK-ADAM models, the gastric emptying time in virtual populations was modified from the default values of 0.4 hours in fasted and 1 hour in fed to the maximal values of 2 and 4 hours, respectively, to sufficiently adapt clinically observed time to reach maximum plasma concentration (t_{max}; 4–6 hours) (http://www.accessdata.fda.gov/drugsatfda_docs/nda/2012/203341Orig1s000ClinPharmR.pdf). It has been reported that the mean gastric emptying time was 15.3 ± 4.7 hours (4.3–20 hours) in healthy subjects (n = 19) following the standard high-fat meal recommended by the FDA guidance (Koziolek et al., 2015). In the F_{oral} and DDI studies, the study outlines of all simulation were on the basis of the clinical study designs described above. For model application, a single oral dose of bosutinib 500 mg was administered to a virtual population of healthy volunteers on day 5 with and without 16-day repeated oral administration of dual CYP3A/P-glycoprotein inhibitors, itraconazole (200 mg once daily) and verapamil (80 mg three times a day).

DDI Prediction on P-gp. Regarding DDIs on intestinal P-gp-mediated efflux, ketoconazole was assumed to inhibit P-gp-mediated efflux in a competitive manner. The reported ketoconazole in vitro IC_{50} values against P-gp varied ~200-fold (a median of 2.0 μM with a range of 0.24–49 μM using various substrates) or ~11-fold (a median of 1.5 μM with a range of 0.42–4.6 μM using digoxin as a substrate) in the Metabolism and Transport Drug Interaction Database (DIDB; School of Pharmacy, University of Washington, Seattle, WA). Therefore, the SAO for ketoconazole inhibition constant (K_i) were performed with PBPK-ADAM models to adequately recover clinical DDI results. Rifampin was assumed to increase intestinal P-gp abundances in PBPK-ADAM models since it was reported that multiple-dose administration of rifampin increased the intestinal P-gp abundances by 3.5-fold, similar to the 4.5-fold for intestinal CYP3A4 (Greiner et al., 1999). Another report also indicated that multiple-dose administration of rifampin increased intestinal P-gp expression (mRNA) and abundance (protein) by 3- and 8-fold, respectively (Giessmann et al., 2004). However, there is no function in Simcyp for precipitant drug-mediated increases in P-gp abundances. Therefore, SFs for P-gp J_{max} were assumed to increase with increasing intestinal P-gp abundances by rifampin-mediated induction. This also assumed that increases in intestinal P-gp abundances were proportional to increases in P-gp-mediated efflux activities. Accordingly, the SAO for P-gp J_{max}

TABLE 2

Outlines of bosutinib PBPK modeling for model refinement, verification, and application

PBPK Model[a]	Approach	Bosutinib Dose (mg)	Precipitant Drug	Clinical Studies Used	Key Parameters Explored
IV	Refinement	120[b]	—	F_{oral}	CL_{int} and V_{ss}
F_a	Refinement	500	—	F_{oral}	$f_{u,gut}$
	Verification	100 and 500	Ketoconazole	DDI	$C_{max}R$ and AUCR
		500	Rifampin	DDI	$C_{max}R$ and AUCR
ADAM	Refinement	500	—	F_{oral}	P-gp kinetics (J_{max} SF)[c]
		100 and 500	—	DDI[d]	P-gp kinetics (J_{max} SF)[c]
	Verification	100 and 500	Ketoconazole	DDI	P-gp inhibition (K_i)[e]
		500	Rifampin	DDI	P-gp induction (abundance)[f]
	Application	500	Itraconazole	—	DDI prediction
		500	Verapamil	—	DDI prediction

—, not applicable.

[a]PBPK model without absorption model (PBPK-IV), PBPK model with the first order absorption model (PBPK-F_a), and PBPK model with the ADAM model using P-gp kinetic parameters (PBPK-ADAM).

[b]Single intravenous 1-hour infusion.

[c]In vitro-to-in vivo scaling factor (SF) for intestinal P-gp J_{max}.

[d]Control groups (bosutinib alone) of the DDI study with ketoconazole (100 and 500 mg) and rifampin (500 mg).

[e]Ketoconazole K_i for intestinal P-gp.

[f]Rifampin-mediated increases in intestinal P-gp abundance.

SFs (for rifampin-mediated P-gp induction) were performed to adequately recover clinical results.

For bosutinib DDI predictions, the vendor-verified compound files in Simcyp library were used, i.e., ketoconazole (sim-ketoconazole 400 mg QD), rifampin (sv-rifampicin-md), itraconazole (sv-itraconazole_fed capsule), itraconazole metabolite (sv-OH-itraconazole), verapamil (sv-verapamil), and verapamil metabolite (sv-norverapamil). The input parameters on CYP3A4-mediated DDIs in these compound files were as follows: ketoconazole competitive $K_i = 0.015$ μM ($f_{u,mic} = 0.97$); rifampin induction $E_{max} = 16$, $EC_{50} = 0.32$ μM, and competitive $K_i = 15$ μM ($f_{u,mic} = 1$), itraconazole competitive $K_i = 0.0013$ μM ($f_{u,mic} = 1$); itraconazole metabolite competitive $K_i = 0.0023$ μM ($f_{u,mic} = 1$); verapamil mechanism-based inhibition $K_I = 2.21$ μM ($f_{u,mic} = 1$) and maximal inactivation rate (k_{inact}) = 2 hour^{-1}; verapamil metabolite mechanism-based inhibition $K_I = 10.3$ μM ($f_{u,mic} = 1$) and $k_{inact} = 18$ hour^{-1}. The input parameters of intestinal P-kinetics were as follows: verapamil $K_m = 0.734$ μM ($f_{u,mic} = 1$), $J_{max} = 2.814$ pmol/min, and (inhibition constant) $K_i = 0.16$ μM ($f_{u,mic} = 1$); verapamil metabolite $K_i = 0.04$ μM ($f_{u,mic} = 1$). For itraconazole-mediated P-gp inhibition, no P-gp inhibition parameters were incorporated into the default compound file; therefore, on the basis of the reported values (a median of 1.7 μM with a range of 0.45–6.7 μM using digoxin as a substrate) in the DIDB, the lower end of itraconazole P-gp K_i values was used as the input parameter (i.e., 0.5 μM). P-gp K_i value of verapamil (0.16 μM) in the default compound file was also near the lower end of reported values (a median 4.9 μM with a range of 0.06–57 μM using digoxin as a substrate with an exception of 224 μM) in the DIDB.

Data Analysis

Pharmacokinetic parameters such as C_{max}, t_{max}, and AUC from time zero to infinity, C_{max} ratio ($C_{max}R$) and AUC ratio ($AUCR$) in treatment groups relative to control groups were obtained from Simcyp outputs. To evaluate predictive model performance, the ratios of predicted-to-observed pharmacokinetic parameters (P/O) were calculated according to the following equation:

$$P/O = \frac{Predicted\ Parameters}{Observed\ Parameters}$$

To assess the predictive model performance, the P/O ratios within ±50% of the observed results (i.e., 0.67–1.5) were provisionally considered to be acceptable as the predefined criteria (Guest et al., 2011; Sager et al., 2015).

Results

Bosutinib PBPK Models without P-gp Kinetics

Model Refinement on Intravenous Pharmacokinetics. On the basis of the intravenous plasma concentration-time profiles in healthy subjects at a dose of 120 mg, we compared the predictive performance of the PBPK models between two different parameter sets, i.e., CL_{int} of

300 μl/min per milligram protein and V_{ss} of 15 l/kg used in the previous model and CL_{int} of 560 μl/min per milligram protein and V_{ss} of 28 l/kg obtained from the F_{oral} study. The intravenous plasma concentration-time profiles were overpredicted by the PBPK model with the parameters used in the previous model (Fig. 1A), resulting in C_{max} and AUC values higher than the observed values with P/O ratios of 1.9 and 1.5, respectively (Table 3). In contrast, the predicted P/O ratio for AUC was within ~10% of the observed values in the PBPK model with the parameters from the F_{oral} study, whereas that for C_{max} (~60%) was close to the acceptable range (≤ ±50%) (Fig. 1B; Table 3). Accordingly, the PBPK model was refined with the CL_{int} of 560 μl/min per milligram protein and the V_{ss} of 28 l/kg obtained from the F_{oral} study.

Model Refinement on Oral Pharmacokinetics. The oral plasma concentration-time profiles of bosutinib in healthy subjects at a dose of 500 mg were predicted by the refined PBPK-F_a model with fixed F_a of 0.7 and $f_{u,gut}$ of 1 used in the previous PBPK model. The PBPK-F_a model considerably underpredicted the plasma concentration-time profiles (Fig. 1C), resulting in that the predicted C_{max} and AUC values were ≥ 2-fold lower than the observed values (Table 3). Since bosutinib F_a was estimated at 0.7 in the mass-balance study, the SAO for $f_{u,gut}$ ranging from 0.01 to 1 was performed to investigate the effect of $f_{u,gut}$ on overall outcomes, particularly, a fraction of the dose that escapes intestinal first-pass metabolism (F_g). Results showed that the plasma concentration-time profiles were reasonably predicted by the PBPK-F_a models with $f_{u,gut}$ of 0.01–0.1 (≤20% difference in AUC). Accordingly, $f_{u,gut}$ was assumed to be comparable to $f_{u,plasma}$ of 0.063 (Fig. 1D; Table 3). The difference between $f_{u,gut}$ of 0.063 and 1 resulted in an approximately 2-fold difference in the predicted F_g (median) of 0.93 and 0.45, respectively.

Model Verification on DDI Outcomes. Bosutinib single-dose DDIs with ketoconazole and rifampin were predicted by the refined PBPK-F_a models with $f_{u,gut}$ of 0.063. The F_a value was set at 0.7 at bosutinib dose of 500 mg, whereas it was calculated at 0.3 at doses of 100 mg on the basis of a comparison of AUC estimates between 100 and 500 mg. The predicted C_{max} and AUC were within ±40% of the observed results in control groups (bosutinib alone) from these three DDI studies (Tables 4–6). In contrast, at bosutinib 100 mg with ketoconazole, the PBPK-F_a model considerably underpredicted the plasma concentrations of bosutinib in the treatment group (bosutinib with ketoconazole), with the P/O ratios of 0.5 for both C_{max} and AUC (Table 4). The P/O ratios for $C_{max}R$ and AUCR were approximately 0.6. Thus, the PBPK-F_a model significantly underpredicted the effect of ketoconazole on bosutinib
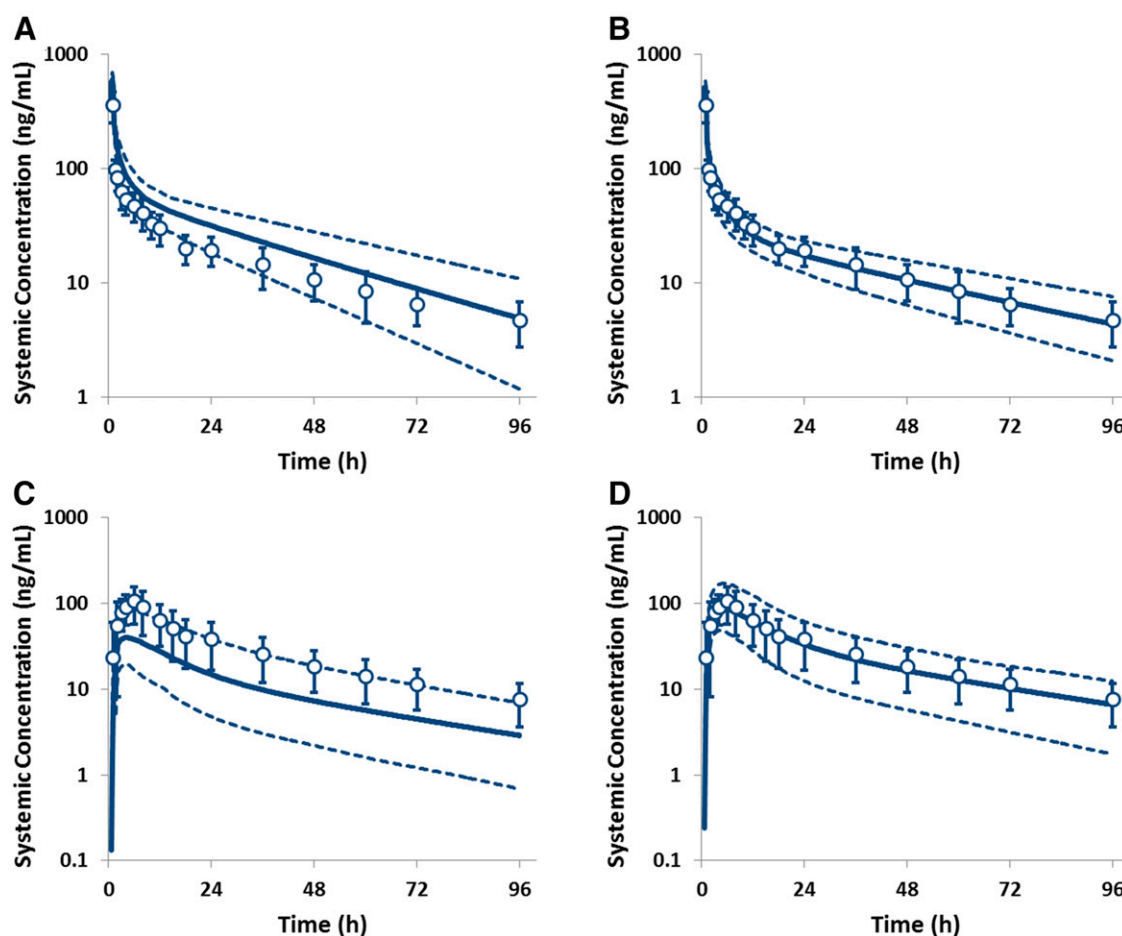
Fig. 1. Clinically observed and PBPK model-predicted plasma concentrations of bosutinib in healthy subjects after a single intravenous and oral administration. Bosutinib was administered intravenously (120 mg, 1-hour infusion) and orally (500 mg) to healthy subjects in a single-dose crossover study. Bosutinib plasma concentrations were predicted in a virtual population of healthy subjects with PBPK-F_a models. Input parameters of bosutinib PBPK models were CL_{int} of 300 μl/min per milligram protein and V_{ss} of 15 l/kg (A) or CL_{int} of 560 μl/min per milligram protein and V_{ss} = 28 l/kg (B–D) with $f_{u,gut}$ of 1 (C) or 0.063 (D). The observed and predicted plasma concentrations are expressed as mean ± S.D. (○) and mean (—) with 5th and 95th percentiles (---), respectively.

exposures at a dose of 100 mg (Fig. 2A). At bosutinib 500 mg with ketoconazole, the PBPK-F_a model tended to underpredict the plasma concentrations of bosutinib in the treatment group with P/O ratios of 0.70 and 0.88 for C_{max} and AUC, respectively (Fig. 2B; Table 5). The P/O ratios of $C_{max}R$ and AUCR were 0.97 and 0.66, respectively. Thus, the underprediction was more pronounced at a dose of 100 mg than 500 mg in the DDI studies with ketoconazole. At bosutinib 500 mg with rifampin, the PBPK-F_a model significantly overpredicted the plasma concentrations of bosutinib with rifampin, resulting in the P/O ratios of 1.6 for C_{max} and 2.4 for AUC (Fig. 2C; Table 6). The predicted $C_{max}R$ and AUCR were approximately 2-fold higher than the observed ratios, i.e., the P/O ratios of 1.9 for both $C_{max}R$ and AUCR.

In these DDI predictions, the predicted F_h values in control groups were approximately 0.6 (median), which increased to near-unity (~1.0) by ketoconazole-mediated CYP3A4 inhibition and decreased to ~0.1 by rifampin-mediated CYP3A4 induction. Thus, the modeling results suggested that hepatic metabolism of bosutinib was near-completely inhibited by ketoconazole or induced by rifampin. The predicted F_g values (~0.9) in control groups also increased to near-unity (~1.0) by ketoconazole, suggesting that the contribution of intestinal metabolism to systemic DDIs was minimal. The predicted F_g values in the DDI study with rifampin decreased to ~0.6, which appeared to be constrained by the faster CYP3A4 degradation rates in intestine (0.03 hour^{-1}) than liver (0.0193 hour^{-1}) and the small $f_{u,gut}$ (0.063) optimized by the

aforementioned SAO. Overall, the modeling results suggested that the predicted changes in bosutinib F_h and F_g by ketoconazole and rifampin could not sufficiently recover the observed DDI results. Therefore, these precipitant drugs could possibly impact the extent of bosutinib absorption (F_a) through P-gp-mediated efflux in intestine.

Bosutinib PBPK Models with P-gp Kinetics

Model Refinement on Oral Pharmacokinetics. To incorporate bosutinib P-gp kinetics into the intestinal absorption process, the PBPK-ADAM models were used with the refined bosutinib parameters. For bosutinib P-gp kinetic parameters, in vitro K_m (0.38 μM) and J_{max} (15 pmol/min) determined in Caco-2 cells were initially incorporated into the PBPK-ADAM models. Clinical studies used for the model refinement were an oral group of bosutinib F_{oral} study at a dose of 500 mg and control groups of DDI studies with ketoconazole (100 and bosutinib 500 mg) and rifampin (bosutinib 500 mg).

The model-predicted plasma concentration-time profiles of bosutinib in control group at a dose of 100 mg were considerably overpredicted by the PBPK-ADAM model with P-gp inputs, resulting in P/O ratios of 4.5 and 2.0 for C_{max} and AUC, respectively (Supplemental Fig. S1A; Table 4). The predicted F_a was approximately 0.7 (median). Compared with the predicted results by the PBPK-ADAM model without P-gp kinetics, the overprediction was slightly improved from the P/O ratios of

was ~3-fold lower than that (~0.7) by the PBPK-ADAM model with an SF of unity.

At bosutinib dose of 500 mg, the PBPK-ADAM model with J_{max} SF of unity sufficiently predicted the plasma concentration-time profiles of bosutinib in an oral group of bosutinib F_{oral} study and control groups of bosutinib 500 mg DDI studies (Supplemental Fig. S1). The P/O ratios were 1.1–1.2 for C_{max} and 1.0–1.4 for AUC (Tables 3, 5, and 6). The model performance was slightly improved from the PBPK-ADAM model without P-gp parameters (P/O ratios of 1.3–1.4 for C_{max} and 1.1–1.6 for AUC). Thus, the effects of intestinal P-gp-mediated efflux on bosutinib exposures could be minimal at the clinically recommended dose of 500 mg. The SAO for J_{max} suggested that the predictive model performance could be improved further to P/O ratios of 0.95–1.0 for C_{max} and 0.94–1.2 for AUC when J_{max} SF was set at 2 in the F_{oral} study and at 4 in the DDI studies (Supplemental Fig. S2; Tables 3, 5, and 6). Subsequently, J_{max} SF of 4 was used for the following model verification on the basis of DDI results. The difference in bosutinib exposures at a dose of 500 mg among these studies could be considered to be within the variability between clinical studies including interindividual variability. The predicted F_a in these studies was 0.5–0.7, which was comparable to the estimated F_a of 0.7 in the mass-balance study.

Model Verification on DDI Outcomes. The DDI prediction of bosutinib with ketoconazole was performed by the PBPK-ADAM models with the optimized J_{max} SFs at doses of 100 and 500 mg. As suggested by the PBPK-F_a modeling results, the effect of ketoconazole on bosutinib exposures was underpredicted by the PBPK-ADAM model without ketoconazole-mediated P-gp inhibition (Fig. 3A and C), particularly at a dose of 100 mg. The P/O ratios for $C_{max}R$ and AUCR were 0.47 and 0.66, respectively, at 100 mg (Table 4), whereas those were 0.72 and 0.60, respectively, at 500 mg (Table 5). The predicted F_h and F_g in control groups increased to near-unity in treatment groups with ketoconazole. Thus, the modeling results suggested that the hepatic and intestinal metabolism of bosutinib was near-completely inhibited by ketoconazole; yet the PBPK-ADAM models underpredicted the effect of

TABLE 3

Clinically observed and PBPK model-predicted pharmacokinetic parameters of bosutinib in humans following a single intravenous and oral administration of bosutinib

Data are expressed as geometric mean with percent coefficient of variation (CV%) in parentheses (n = 13–14 for the observed; n = 6 per group × 6 groups for the predicted) except for median t_{max} with minimal to maximal values.

Dose	PBPK Model[a]	J_{max}[b]	Analysis[c]	C_{max}	t_{max}	AUC
mg		SF		ng/ml	h	ng·h/ml
120	—	—	Obs	347 (28)	1 (1–1)	1920 (26)
	IV-1	—	Pred	662 (14)	1 (1–1)	2934 (35)
			P/O	1.91	—	1.53
	IV-2	—	Pred	563 (13)	1 (1–1)	2128 (28)
			P/O	1.62	—	1.11
500	—	—	Obs	109 (43)	6 (2–8)	2736 (44)
	F_a-1	—	Pred	36 (55)	4 (3–7)	1012 (77)
			P/O	0.33	—	0.37
	F_a-2	—	Pred	83 (47)	4 (3–7)	2374 (46)
			P/O	0.76	—	0.87
	ADAM	—	Pred	138 (48)	5 (2–11)	3038 (64)
			P/O	1.27	—	1.11
		1	Pred	123 (49)	5 (2–15)	2770 (66)
			P/O	1.12	—	1.01
		2	Pred	112 (51)	5 (2–17)	2560 (68)
			P/O	1.03	—	0.94
		4	Pred	96 (53)	5 (2–20)	2235 (71)
			P/O	0.88	—	0.82

—, not application or not calculated.

[a]CL_{int} = 300 μl/min per milligram protein and V_{ss} = 15 l/kg (IV-1) or CL_{int} = 560 μl/min per milligram protein and V_{ss} = 28 l/kg (IV-2, F_a-1, F_a-2, and ADAM) with $f_{u,gut}$ = 1 (F_a-1) or 0.063 (F_a-2 and ADAM).

[b]Predicted in vitro-to-in vivo scaling factor (SF) for intestinal P-gp J_{max}.

[c]Obs, observed; Pred, predicted; P/O, ratios of predicted to observed value.

5.4 and 2.2 for C_{max} and AUC, respectively (Table 4). Following the SAO for J_{max} SFs in PBPK-ADAM models, the predicted C_{max} and AUC with an SF of 25 were within ±20% of the observed results (Supplemental Fig. S2A; Table 4). The predicted F_a was ~0.3, which

TABLE 4

Clinically observed and PBPK model-predicted pharmacokinetic parameters of bosutinib in bosutinib 100-mg single-dose DDI studies with ketoconazole

Data are expressed as mean with percent coefficient of variation (CV%) in parentheses (n = 24 for the observed; n = 6 per group × 6 groups for the predicted) except for median t_{max} with minimal to maximal values and geometric mean for $C_{max}R$ and AUCR with 90% confidence interval.

Group[a]	PBPK Model	J_{max}[b]	K_i[c]	Analysis[d]	C_{max}	AUC	$C_{max}R$[e]	AUCR[e]
		SF	μM		ng/ml	ng·h/ml	ratio	ratio
Control	—	—	—	Obs	7.0 (45)	323 (43)	—	—
	F_a	—	—	Pred	7.2 (45)	265 (68)	—	—
				P/O	1.03	0.82	—	—
	ADAM	—	—	Pred	38 (44)	709 (68)	—	—
				P/O	5.41	2.19	—	—
		1	—	Pred	31 (47)	653 (72)	—	—
				P/O	4.47	2.02	—	—
		25	—	Pred	8.0 (86)	276 (95)	—	—
				P/O	1.15	0.85	—	—
Test	—	—	—	Obs	38 (54)	2631 (30)	5.2 (4.3–6.2)	8.6 (7.5–9.9)
	F_a	—	—	Pred	20 (39)	1221 (88)	2.9 (2.6–3.2)	4.7 (3.7–5.7)
				P/O	0.53	0.46	0.57	0.55
	ADAM	25	—	Pred	21 (77)	1494 (85)	2.5 (2.3–2.9)	5.7 (5.3–8.1)
				P/O	0.56	0.57	0.47	0.66
		25	0.2	Pred	37 (56)	2098 (78)	5.2 (4.6–5.7)	11 (9.3–14)
				P/O	0.96	0.80	1.00	1.32

—, not applicable or not calculated.

[a]Bosutinib 100 mg without and with ketoconazole 400 mg once daily (control and test groups, respectively).

[b]Predicted in vitro-to-in vivo scaling factor (SF) for intestinal P-gp J_{max}.

[c]Predicted ketoconazole K_i value for intestinal P-gp.

[d]Obs, observed; Pred, predicted; P/O, ratios of predicted to observed value.

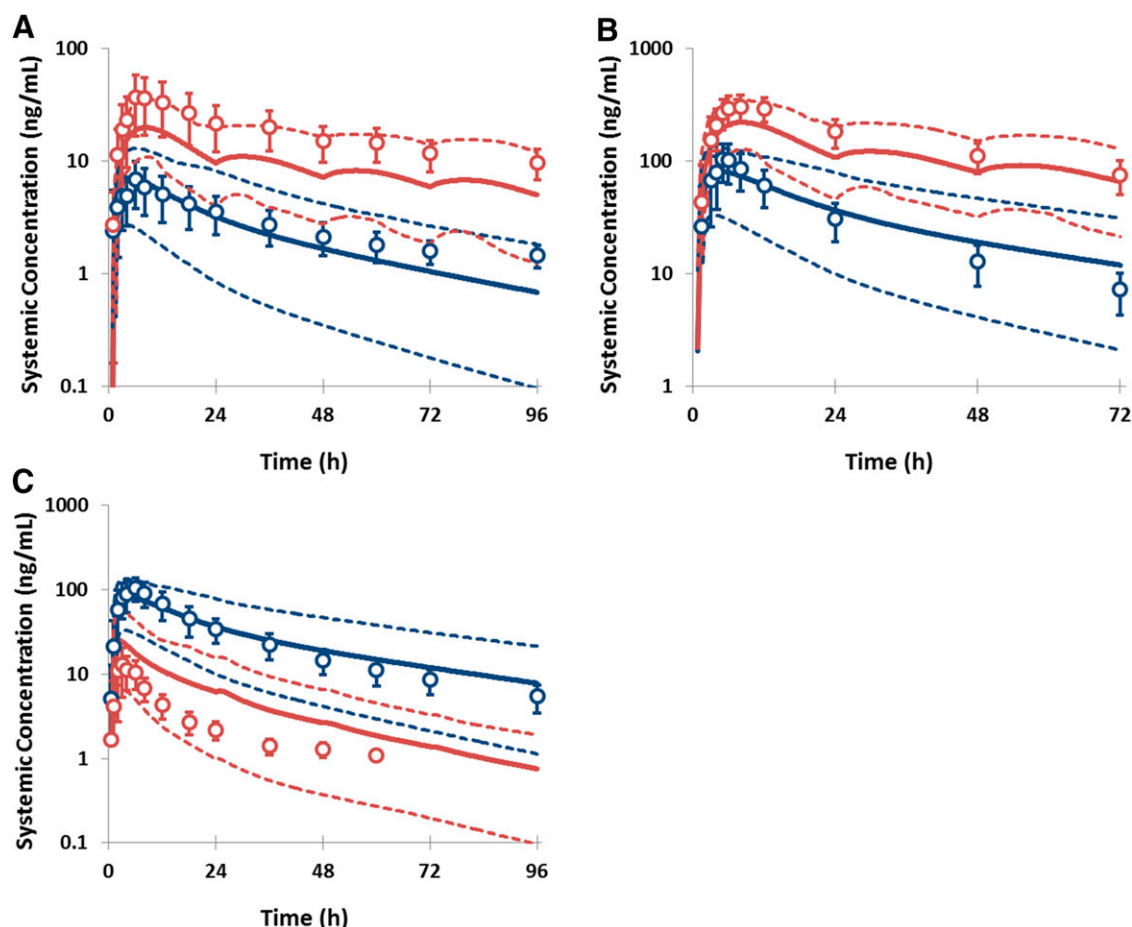[e]Ratios of C_{max} and AUC in test group relative to control group.

Fig. 2. Clinically observed and PBPK model-predicted plasma concentrations of bosutinib in healthy subjects after a single oral administration of bosutinib with and without coadministration of ketoconazole and rifampin. A single oral dose of bosutinib was administered to healthy subjects at a dose of 100 mg (A) or 500 mg (B and C) with and without repeated coadministration of ketoconazole 400 mg once daily (A and B) or rifampin 600 mg once daily (C). Bosutinib plasma concentrations were predicted in a virtual population of healthy subjects with PBPK-F_a models. The observed and predicted plasma concentrations are expressed as mean ± S.D. (○) and mean (—) with 5th and 95th percentiles (---), respectively.

ketoconazole on bosutinib exposures. Accordingly, ketoconazole K_i for P-gp was incorporated into the PBPK-ADAM models to account for ketoconazole-mediated P-gp inhibition. Following the SAO for ketoconazole K_i, the predicted C_{max} and AUC by PBPK-ADAM models with K_i values of 0.1–0.3 μM were in the acceptable range (≤±50%) of the observed results in the treatment group at a 100-mg bosutinib dose. When K_i was set at 0.2 μM, the predicted C_{max} and AUC were within ± 25% of the observed results, resulting in the P/O ratios for C_{max}R and AUCR of 1.0 and 1.3, respectively (Fig. 3B; Table 4). Bosutinib F_a (median) was predicted to increase from 0.2 to 0.4. Assuming the general hypothesis that K_i was intrinsic, the effect of ketoconazole on bosutinib oral exposures at a dose of 500 mg was predicted by the PBPK-ADAM models with ketoconazole K_i of 0.2 μM. The predicted C_{max} and AUC were within ≤ ±25% of the observed values, resulting in the P/O ratios for C_{max}R and AUCR of 0.87 and 0.70, respectively (Fig. 3D; Table 5). Compared with the predicted results without ketoconazole K_i, the DDI prediction was slightly improved from the P/O ratios for C_{max}R of 0.72 and AUCR of 0.60. Bosutinib F_a (median) was predicted to increase from 0.5 to 0.7 at 500 mg by ketoconazole-mediated P-gp inhibition.

The DDI prediction of bosutinib with rifampin was also performed by the PBPK-ADAM model with the optimized intestinal P-gp J_{max} SF. The PBPK-ADAM model considerably underpredicted the effect of rifampin on bosutinib exposures even though the predicted F_h and

F_g markedly decreased to 0.11 and 0.64, respectively (Fig. 4A). The P/O ratios for C_{max} and AUC were 2.6–3.0, resulting in the P/O ratios of 2.5–2.8 for C_{max}R and AUCR (Table 6). The increases in intestinal P-gp abundances were therefore incorporated into PBPK-ADAM models to account for rifampin-mediated P-gp induction, as was suggested by the PBPK-F_a modeling results. Following the SAO for J_{max} SFs as rifampin-mediated fold-increases in P-gp abundances, the predicted C_{max} and AUC were in the acceptable range (≤±50%) of the observed results in treatment group whose J_{max} SFs were set at 32–48 to correspond to the P-gp induction of 8- to 12-fold on top of an SF of 4 used for control group (Supplemental Table S1). Assuming the fold-increase in P-gp abundance of 10, the C_{max} and AUC were within ±30% of the observed values, resulting in P/O ratios for C_{max}R and AUCR of 0.86 and 0.95, respectively (Fig. 4B; Table 6). Bosutinib F_a was predicted to decrease from 0.6 to 0.2 by rifampin-mediated P-gp induction.

Model Application to DDI Prediction. Bosutinib DDIs with dual CYP3A/P-gp inhibitors itraconazole and verapamil were predicted by the PBPK-ADAM models. In these DDI predictions, a single oral dose of bosutinib 500 mg was administered to a virtual population of healthy volunteers on day 5 with and without 16-day repeated oral administration of either itraconazole (200 mg one daily) or verapamil (80 mg three times a day). The predicted C_{max}R and AUCR were, respectively, 2.0 and 8.5 with itraconazole and 2.0 and 5.1 with verapamil (Table 7).

TABLE 5

Clinically observed and PBPK model-predicted pharmacokinetic parameters of bosutinib in bosutinib 500-mg single-dose DDI studies with ketoconazole

Data are expressed as mean with percent coefficient of variation (CV%) in parentheses (n = 54–56 for the observed; n = 6 per group × 6 groups for the predicted) except for median t_{max} with minimal to maximal values and geometric mean for $C_{max}R$ and AUCR with 90% confidence interval.

Group[a]	PBPK Model	J_{max}[b] SF	K_i[c] μM	Analysis[d]	C_{max} ng/ml	AUC ng·h/ml	$C_{max}R$[e] ratio	AUCR[e] ratio
Control	—	—	—	Obs	114 (35)	2330 (35)	—	—
	F_a	—	—	Pred	84 (41)	3013 (64)	—	—
				P/O	0.74	1.29	—	—
	ADAM	—	—	Pred	153 (48)	3606 (64)	—	—
				P/O	1.34	1.55	—	—
		1	—	Pred	136 (49)	3316 (66)	—	—
				P/O	1.20	1.42	—	—
		4	—	Pred	109 (53)	2738 (71)	—	—
				P/O	0.95	1.18	—	—
Test	—	—	—	Obs	326 (24)	15,200 (29)	2.9	6.5
	F_a	—	—	Pred	228 (32)	13,311 (69)	2.8 (2.5–3.1)	4.2 (3.3–5.2)
				P/O	0.70	0.88	0.97	0.66
	ADAM	4	—	Pred	226 (43)	10,639 (61)	2.1 (2.0–2.3)	4.0 (3.1–4.9)
				P/O	0.69	0.70	0.72	0.60
		4	0.2	Pred	272 (40)	12,127 (57)	2.6 (2.4–2.8)	4.7 (3.7–5.7)
				P/O	0.83	0.80	0.87	0.70

—, not applicable or not calculated.
[a]Bosutinib 500 mg without and with ketoconazole 400 mg once daily (control and test groups, respectively).
[b]Predicted in vitro-to-in vivo scaling factor (SF) for intestinal P-gp J_{max}.
[c]Predicted ketoconazole K_i value for intestinal P-gp.
[d]Obs, observed; Pred, predicted; P/O, ratios of predicted to observed value.
[e]Ratios of C_{max} and AUC in test group relative to control group.

Compared with the DDI prediction without P-gp inhibition (i.e., only CYP3A inhibition), the differences in $C_{max}R$ and AUCR were negligible to minimal. These results together with the DDI prediction with ketoconazole suggested minimal impacts of P-gp-mediated efflux on bosutinib DDIs with P-gp inhibitors at clinically recommended dose of bosutinib 500 mg.

Discussion

Utilizing PBPK modeling for understanding pharmacokinetic mechanism of NMEs has become common practice in drug development as well as regulatory decision-making (Rowland et al., 2011; Huang and Rowland, 2012; Prueksaritanont et al., 2013; Wagner et al., 2015, 2016; Shebley et al., 2018). Modeling approaches typically consist of three

TABLE 6

Clinically observed and PBPK model-predicted pharmacokinetic parameters of bosutinib in bosutinib 500-mg single-dose DDI studies with rifampin

Data are expressed as mean with percent coefficient of variation (CV%) in parentheses (n = 22–24 for the observed; n = 6 per group × 6 groups for the predicted) except for median t_{max} with minimal to maximal values and geometric mean for $C_{max}R$ and AUCR with 90% confidence interval.

Group[a]	PBPK Model	J_{max}[b] SF	Induction[c] fold	Analysis[d]	C_{max} ng/ml	AUC ng·h/ml	$C_{max}R$[e] ratio	AUCR[e] ratio
Control	—	—	—	Obs	112 (26)	2740 (29)	—	—
	F_a	—	—	Pred	83 (40)	3005 (65)	—	—
				P/O	0.74	1.10	—	—
	ADAM	—	—	Pred	153 (48)	3606 (64)	—	—
				P/O	1.37	1.32	—	—
		1	—	Pred	136 (49)	3316 (66)	—	—
				P/O	1.22	1.21	—	—
		4	—	Pred	109 (53)	2738 (71)	—	—
				P/O	0.97	1.00	—	—
Test	—	—	—	Obs	16 (42)	207 (22)	0.14 (0.12–0.16)	0.08 (0.07–0.09)
	F_a	—	—	Pred	26 (71)	487 (76)	0.27 (0.23–0.31)	0.14 (0.12–0.17)
				P/O	1.62	2.35	1.92	1.86
	ADAM	4	—	Pred	41 (64)	628 (89)	0.34 (0.30–0.38)	0.21 (0.18–0.24)
				P/O	2.56	3.03	2.46	2.84
		4	10	Pred	16 (64)	260 (106)	0.13 (0.11–0.15)	0.08 (0.06–0.09)
				P/O	1.01	1.26	0.86	0.95

—, not applicable or not calculated.
[a]Bosutinib 500 mg without and with rifampin 600 mg once daily (control and test groups, respectively).
[b]Predicted in vitro-to-in vivo scaling factor (SF) for intestinal P-gp J_{max}.
[c]Predicted rifampin-mediated fold increase in intestinal P-gp.
[d]Obs, observed; Pred, predicted; P/O, ratios of predicted to observed value.
[e]Ratios of C_{max} and AUC in test group relative to control group.
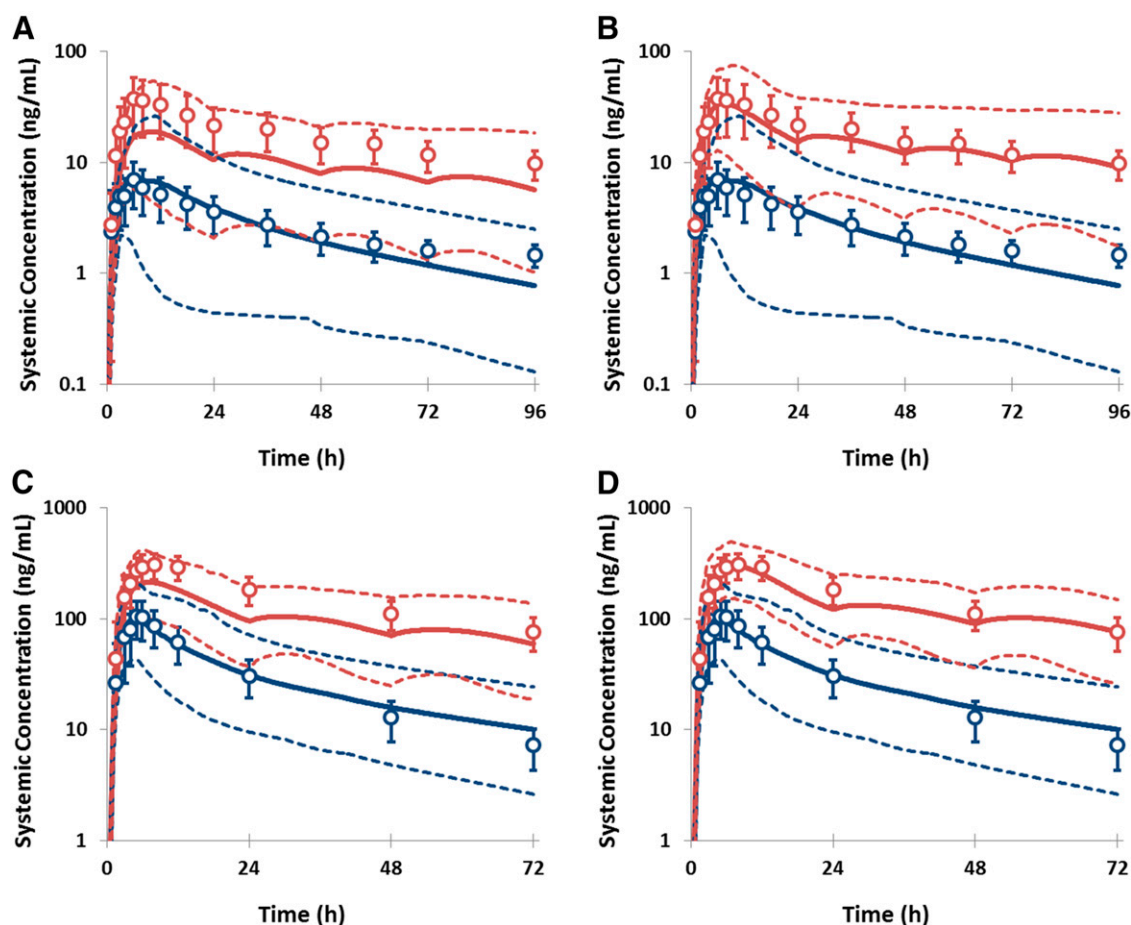
Fig. 3. Clinically observed and PBPK model-predicted plasma concentrations of bosutinib in healthy subjects after a single oral administration of bosutinib with and without coadministration of ketoconazole. A single oral dose of bosutinib was administered to healthy subjects at a dose of 100 mg (A and B) or 500 mg (C and D) with and without repeated coadministration of 400 mg ketoconazole once daily. Bosutinib plasma concentrations were predicted in a virtual population of healthy subjects with PBPK-ADAM models. Input parameters of P-gp kinetic parameters in PBPK models were bosutinib K_m of 0.38 μM and J_{max} of 15 pmol/min with J_{max} SFs of 25 (A and B) or 4 (C and D) without ketoconazole K_i (A and C) or with ketoconazole K_i of 0.2 μM (B and D). The observed and predicted plasma concentrations are expressed as mean $\pm$ S.D. (○) and mean (—) with 5th and 95th percentiles (---), respectively.

main tiers: model development, verification, and application. Subsequently, it is critical to continuously verify and refine PBPK models, if necessary, on the basis of latest available data. Accordingly, we have refined the previously developed bosutinib PBPK model with the latest F_{oral} results. Apparently, the present PBPK model could rationalize the underlying DDI mechanisms with ketoconazole and rifampin through not only CYP3A4 but also P-gp. However, the present study undoubtedly highlighted the challenges of PBPK modeling for P-gp substrate drugs. Some potential issues raised in the present study therefore remain and warrant further discussion.

One of the most important pharmacokinetic parameters for oral drugs is F_{oral} ($F_a \times F_g \times F_h$). Bosutinib F_{oral} and F_h were estimated at ~0.3 and ~0.5, respectively, in the F_{oral} study, and F_a was estimated at ~0.7 in the mass-balance study at a dose of 500 mg. Subsequently, the calculated F_g was ~0.9 from F_{oral} (~0.3), F_a (~0.7), and F_h (~0.5). Thus, the F_{oral} result was valuable in the verification of the PBPK models. However, the refined PBPK-F_a models underpredicted the effects of ketoconazole and rifampin on bosutinib exposures. In both cases, the observed DDI results could not be recovered sufficiently by the model-predicted changes in bosutinib F_g and F_h as mentioned before, suggesting that bosutinib F_a could possibly be altered by these precipitant drugs through P-gp–mediated efflux. Consistently, the increases in bosutinib exposures estimated as C_{max} and AUC were supraproportional at the lower doses of

50–200 mg and approximately dose-proportional at the higher doses of 200–600 mg (http://www.accessdata.fda.gov/drugsatfda_docs/nda/2012/203341Orig1s000ClinPharmR.pdf). In contrast, the observed terminal half-lives (13–22 hours) were comparable across the doses, suggesting the linear elimination (e.g., hepatic clearance) across the doses tested. This finding appeared to be consistent with in vitro metabolism data showing much higher K_m estimates of two major metabolites (8–23 μM for oxydechlorinated and N-desmethyl bosutinib) than the observed unbound steady-state C_{max} of ~0.03 μM (http://www.accessdata.fda.gov/drugsatfda_docs/nda/2012/203341Orig1s000ClinPharmR.pdf). Thus, bosutinib nonlinear pharmacokinetics could possibly result from the dose-dependent increases in F_a owing largely to a saturation of intestinal P-gp efflux.

Two of the most important factors governing F_a are solubility and permeability, including active transports. It has been reported that it would be challenging to accurately predict the F_a of many drugs, particularly basic compounds with low solubility (Zhang et al., 2014; Lin and Wong, 2017; Li et al., 2018). Bosutinib exhibits pH-dependent aqueous solubility, with the solubility decreasing from 21 to 0.038 mM over the pH range of 1 to 6.8. In contrast, bosutinib intestinal concentrations calculated by dose amounts divided by 250 ml were 0.38–3.8 mM at doses of 50–500 mg. Therefore, bosutinib F_a could be limited by solubility, whereas its distinctive pH-dependent solubility could potentially increase its gastrointestinal solubility in vivo. Bosutinib exhibited positive food effects (high-fat meal)
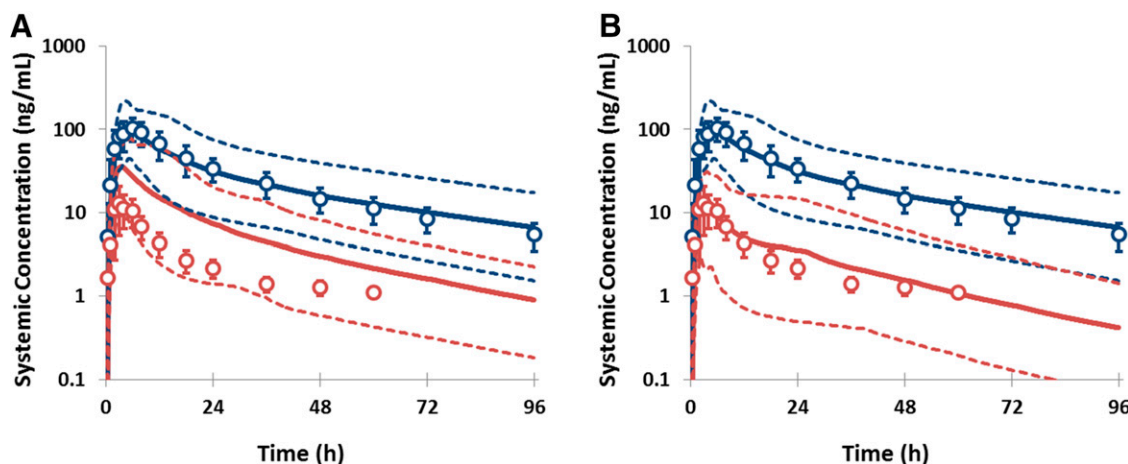
Fig. 4. Clinically observed and PBPK model-predicted plasma concentrations of bosutinib in healthy subjects after a single oral administration of bosutinib with and without coadministration of rifampin. A single oral dose of bosutinib was administered to healthy subjects at a dose of 500 mg with and without repeated coadministration of 600 mg rifampin once daily. Bosutinib plasma concentrations were predicted in a virtual population of healthy subjects with PBPK-ADAM models. Input parameters of P-gp kinetic parameters in bosutinib PBPK models were K_m of 0.38 μM and J_{max} of 15 pmol/min with J_{max} SFs of 4 (A) or 40 (B). The observed and predicted plasma concentrations are expressed as mean $\pm$ S.D. ($\bigcirc$) and mean (—) with 5th and 95th percentiles (---), respectively.

on oral exposures ($\sim$1.6-fold) in healthy volunteers (n = 23 to 24) at a dose of 400 mg (http://www.accessdata.fda.gov/drugsatfda_docs/nda/2012/ 203341Orig1s000ClinPharmR.pdf). The observed positive food effects were sufficiently predicted by the present PBPK-ADAM model showing $\sim$1.5-fold higher exposures in a fed state (high-fat meal) than a fasted state (Supplemental Table S2). Thus, the modeling results suggested that the PBPK-ADAM model could adequately predict the solubility-limited absorption. Bosutinib in vitro passive permeability was moderate ($\sim$7 $\times$ 10^{-6} cm/s), which was on the borderline of the proposed cut-off (5 $\times$ 10^{-6} cm/s) for F_a in the extended clearance classification system (Di et al., 2011; Varma et al., 2012). The relative P-gp distribution increases from proximal to distal small intestine, although expression levels appear slightly higher in jejunum than ileum (Fricker et al., 1996; Mouly and Paine, 2003; Englund et al., 2006; Harwood et al., 2015). Therefore, highly soluble and permeable drugs, even those that are P-gp substrates, can be absorbed rapidly and extensively in duodenum and proximal jejunum. In contrast, P-gp-mediated efflux frequently reduces absorption rate and extent of P-gp substrates with low-to-moderate solubility or permeability. Consistent with this, bosutinib absorption was relatively slow, with the observed median t_{max} of 4–6 hours, and its F_a was incomplete ($\leq$0.7) at the doses

tested. Unbound intracellular enterocyte concentrations calculated by k_a (0.61 hour^{-1}), F_a (1), $f_{u,gut}$ (0.063), and enterocyte blood flow (18 l/h) were 0.2–2.0 μM at a doses of 50–500 mg (Rostami-Hodjegan and Tucker, 2004). When the predicted F_a values (0.3–0.7) were used, the calculated unbound intracellular enterocyte concentrations were 0.06–1.4 μM. In the ADAM model, bosutinib enterocyte concentrations were predicted in each region (subcompartment) of the gastrointestinal tract as a function of time. The predicted maximal concentrations in the subcompartments were 0.1–0.7 and 0.8–2.4 μM at doses of 100 and 500 mg, respectively. Thus, the predicted enterocyte concentrations were in a range comparable to the in vitro K_m (0.38 μM). Collectively, these findings suggested a potential interplay between the pH-dependent solubility, moderate permeability, and P-gp-mediated efflux on bosutinib absorption, as suggested also for other P-gp substrates (Burton et al., 2002; Jamei et al., 2009b; Sjogren et al., 2013).

SAO are powerful tools to assess the effects on overall outputs of uncertainty around input parameters, often leading to model improvement and additional mechanistic insights (Zhao et al., 2012; Shardlow et al., 2013; Shepard et al., 2015). Accordingly, the SAO for bosutinib P-gp kinetic parameters were performed in the present study. First,

TABLE 7

PBPK-ADAM model-predicted pharmacokinetic parameters of bosutinib in bosutinib 500-mg single-dose DDI studies with verapamil and itraconazole

Data are expressed as geometric mean with percent coefficient of variation (CV%) except for C_{max}R and AUCR with 90% confidence interval in parentheses (n = 6 per group $\times$ 6 groups for the predicted).

PBPK Model	Precipitant Drug	Group[a]	K_i[b]	C_{max}	AUC	C_{max}R[c]	AUCR[c]
			μM	ng/ml	$ng \cdot h/ml$	$ratio$	$ratio$
ADAM	Itraconazole	Control	—	114 (51)	2578 (71)	—	—
		Test	—	228 (46)	21,108 (123)	2.0 (1.9–2.1)	8.5 (6.5–10)
			0.5	229 (46)	21,159 (123)	2.0 (1.9–2.1)	8.5 (6.5–10)
	Verapamil	Control	—	112 (49)	2528 (70)	—	—
		Test	—	190 (50)	11,269 (110)	1.7 (1.6–1.8)	4.5 (3.7–5.3)
			0.16	226 (49)	13,015 (111)	2.0 (1.9–2.2)	5.1 (4.3–6.2)

—, not applicable.

[a]Bosutinib 500 mg without and with itraconazole 200 mg once daily (control and test groups, respectively) or verapamil 80 mg three times a day.

[b]K_i for intestinal P-gp.

[c]Ratios of C_{max} and AUC in test group relative to control group.

bosutinib K_m was assumed to be intrinsic and was fixed. Consequently, J_{max} SFs were optimized to adequately recover the observed results. The SAO suggested a dose-dependent decrease in P-gp-mediated C_{Lint} in intestine as a possible explanation for the dose-dependent decrease in SFs at the doses of 100 to 500 mg. The general hypothesis is that J_{max} is consistent across doses. Thus, the difference in J_{max} SFs between the doses suggested that J_{max} SFs could be optimized as *apparent* J_{max} instead of *true* J_{max}. One of the potential reasons could be that PBPK models might not adequately capture the interplay between P-gp-mediated efflux, permeability, and pH-dependent solubility in each region of gastrointestinal tract, e.g., the regional differences in P-gp-meditated CL_{int}. Further model refinement may be required to recover nonlinear pharmacokinetics of bosutinib across doses, suggesting the present PBPK models could be considered to be "fit-for-purpose" models.

Ketoconazole is generally assumed to be an inhibitor only of CYP3A in clinical DDI studies, although ketoconazole is known to inhibit P-gp (Rautio et al., 2006; Vermeer et al., 2016). The reason behind it could probably be the minimal P-gp effects on the absorption of many dual CYP3A and P-gp substrates owing to the saturation of P-gp-mediated efflux at clinical doses. Clinically observed bosutinib $C_{max}R$ and AUCR by ketoconazole was more pronounced at a dose of 100 mg than 500 mg, which appeared to be consistent with the dose-dependent saturation of P-gp-mediated efflux (Tables 4 and 5). To adequately recover the observed DDIs, the SAO indicated a ketoconazole in vivo K_i of 0.1–0.3 μM, which were in line with the lower end of the reported in vitro IC_{50} of ~0.2 μM in the DIDB. The K_i values for itraconazole and verapamil used in the PBPK models were also near the lower end of reported values as noted above. Overall, the PBPK modeling results suggested minimal impact of P-gp-mediated efflux on bosutinib DDIs with P-gp inhibitors at the clinically recommended dose of 500 mg.

Rifampin is well known to be a modulator for not only cytochrome P450 enzymes but also transporter proteins, including P-gp (Haslam et al., 2008; Williamson et al., 2013; Wagner et al., 2016). Following multiple-dose coadministration of rifampin, oral exposures of a P-gp probe substrate, digoxin, decreased by ~2-fold, whereas intravenous exposures were not significantly altered (Novi et al., 1980; Gault et al., 1984; Greiner et al., 1999). Thus, the decrease in oral exposure of digoxin was probably owing to rifampin-mediated P-gp induction in intestine resulting in the decrease in digoxin F_a. Since bosutinib was a dual-substrate of CYP3A4 and P-gp, the decrease in bosutinib exposures by rifampin could possibly be caused by complex DDI mechanisms through not only CYP3A4 but also P-gp. Consistently, the effect of rifampin on bosutinib exposures was considerably underpredicted by the PBPK models when accounting for only rifampin-mediated CYP3A4 induction. The subsequent SAO suggested that the observed DDI results could adequately be recovered by 8- to 12-fold increases in intestinal P-gp abundances by rifampin (Table 6). The predicted fold-increases in intestinal P-gp abundances were comparable to the reported results (Giessmann et al., 2004). The predicted increases in P-gp abundances were also comparable to those in CYP3A4 induction (Almond et al., 2016), which appeared to be consistent with the literature reporting the similar increases in rifampin-mediated CYP3A4 and P-gp expression levels (Greiner et al., 1999). For DDI prediction with CYP3A inducers, efavirenz is frequently used for PBPK modeling as a moderate inducer (Ke et al., 2016; Wagner et al., 2016). However, it has been reported that efavirenz did not induce intestinal P-gp in the clinic (Mouly et al., 2002; Oswald et al., 2012). Provisionally, the results of bosutinib DDI prediction with rifampin, when the different fold-increases in intestinal P-gp abundance (i.e., 1- to 16-fold) are used, could possibly serve as indexes of DDI prediction with CYP3A/P-gp dual inducers (Supplemental Table S1). With P-gp abundances increasing by 16-fold,

bosutinib $C_{max}R$ and AUCR decreased from 0.34 to 0.09 and 0.21 to 0.06, respectively, suggesting some degree of impact of intestinal P-gp induction on bosutinib exposures at the clinically recommended dose of 500 mg.

In summary, the present study demonstrated that bosutinib PBPK models are reasonably refined, as verified on the basis of currently available data. The results suggested that P-gp-mediated intestinal efflux could play a substantial role on bosutinib DDIs with ketoconazole and rifampin. Overall, it may prove critical to incorporate P-gp kinetics in the PBPK models in order to understand the underlying DDI mechanisms for P-gp substrates such as bosutinib, particularly when clinical data exhibit nonlinear pharmacokinetics that could be a result of saturation of intestinal P-gp-mediated efflux.

Authorship Contributions

Participated in research design: Yamazaki.

Performed data analysis: Costales, Kimoto, Yamazaki.

Wrote or contributed to the writing of the manuscript: Costales, Kimoto, Loi, Varma, Yamazaki.

References

Abbas R, Boni J, and Sonnichsen D (2015) Effect of rifampin on the pharmacokinetics of bosutinib, a dual Src/Abl tyrosine kinase inhibitor, when administered concomitantly to healthy subjects. *Drug Metab Pers Ther* **30**:57–63.

Abbas R, Chaudhary I, Hug BA, Leister C, Burns J, Vashishtha S, Erve JCL, and Sonnichsen D (2010) Mass balance, metabolic disposition, metabolite characterization, and pharmacokinetics of oral 14C-labeled bosutinib in healthy subjects. *Drug Metab Rev* **42**:228–229.

Abbas R, Hug BA, Leister C, Burns J, and Sonnichsen D (2011) Effect of ketoconazole on the pharmacokinetics of oral bosutinib in healthy subjects. *J Clin Pharmacol* **51**:1721–1727.

Abbas R, Hug BA, Leister C, and Sonnichsen D (2012) A randomized, crossover, placebo- and moxifloxacin-controlled study to evaluate the effects of bosutinib (SKI-606), a dual Src/Abl tyrosine kinase inhibitor, on cardiac repolarization in healthy adult subjects. *Int J Cancer* **131**: E304–E311.

Almond LM, Mukadam S, Gardner I, Okialda K, Wong S, Hatley O, Tay S, Rowland-Yeo K, Jamei M, Rostami-Hodjegan A, et al. (2016) Prediction of drug-drug interactions arising from CYP3A induction using a physiologically based dynamic model. *Drug Metab Dispos* **44**: 821–832.

Burton PS, Goodwin JT, Vidmar TJ, and Amore BM (2002) Predicting drug absorption: how nature made it a difficult problem. *J Pharmacol Exp Ther* **303**:889–895.

Di Li, Whitney-Pickett C, Umland JP, Zhang H, Zhang X, Gebhard DF, Lai Y, Federico JJ, III, Davidson RE, Smith R, et al. (2011) Development of a new permeability assay using low-efflux MDCKII cells. *J Pharm Sci* **100**:4974–4985.

Englund G, Rorsman F, Rönnblom A, Karlbom U, Lazorova L, Gråsjö J, Kindmark A, and Artursson P (2006) Regional levels of drug transporters along the human intestinal tract: co-expression of ABC and SLC transporters and comparison with Caco-2 cells. *Eur J Pharm Sci* **29**:269–277.

Fricker G, Drewe J, Huwyler J, Gutmann H, and Beglinger C (1996) Relevance of p-glycoprotein for the enteral absorption of cyclosporin A: in vitro-in vivo correlation. *Br J Pharmacol* **118**: 1841–1847.

Gault H, Longerich L, Dawe M, and Fine A (1984) Digoxin-rifampin interaction. *Clin Pharmacol Ther* **35**:750–754.

Giessmann T, Modess C, Hecker U, Zschiesche M, Dazert P, Kunert-Keil C, Warzok R, Engel G, Weitschies W, Cascorbi I, et al. (2004) CYP2D6 genotype and induction of intestinal drug transporters by rifampin predict presystemic clearance of carvedilol in healthy subjects. *Clin Pharmacol Ther* **75**:213–222.

Greiner B, Eichelbaum M, Fritz P, Kreichgauer HP, von Richter O, Zundler J, and Kroemer HK (1999) The role of intestinal P-glycoprotein in the interaction of digoxin and rifampin. *J Clin Invest* **104**:147–153.

Guest EJ, Aarons L, Houston JB, Rostami-Hodjegan A, and Galetin A (2011) Critique of the two-fold measure of prediction success for ratios: application for the assessment of drug-drug interactions. *Drug Metab Dispos* **39**:170–173.

Harwood MD, Achour B, Russell MR, Carlson GL, Warhurst G, and Rostami-Hodjegan A (2015) Application of an LC-MS/MS method for the simultaneous quantification of human intestinal transporter proteins absolute abundance using a QconCAT technique. *J Pharm Biomed Anal* **110**:27–33.

Haslam IS, Jones K, Coleman T, and Simmons NL (2008) Rifampin and digoxin induction of MDR1 expression and function in human intestinal (T84) epithelial cells. *Br J Pharmacol* **154**:246–255.

Hsyu PH, Pignataro DS, and Matschke K (2017) Effect of aprepitant, a moderate CYP3A4 inhibitor, on bosutinib exposure in healthy subjects. *Eur J Clin Pharmacol* **73**:49–56 .

Hsyu PH, Pignataro DS, and Matschke K (2018) Absolute Bioavailability of Bosutinib in Healthy Subjects From an Open-Label, Randomized, 2-Period Crossover Study. *Clin Pharmacol Drug Dev* **7**:373–381.

Huang SM and Rowland M (2012) The role of physiologically based pharmacokinetic modeling in regulatory review. *Clin Pharmacol Ther* **91**:542–549.

Jamei M, Marciniak S, Feng K, Barnett A, Tucker G, and Rostami-Hodjegan A (2009a) The Simcyp population-based ADME simulator. *Expert Opin Drug Metab Toxicol* **5**:211–223.

Jamei M, Turner D, Yang J, Neuhoff S, Polak S, Rostami-Hodjegan A, and Tucker G (2009b) Population-based mechanistic prediction of oral drug absorption. *AAPS J* **11**:225–237.

Jones HM, Chen Y, Gibson C, Heimbach T, Parrott N, Peters SA, Snoeys J, Upreti VV, Zheng M, and Hall SD (2015) Physiologically based pharmacokinetic modeling in drug discovery and development: a pharmaceutical industry perspective. *Clin Pharmacol Ther* **97**:247–262.

Jones H and Rowland-Yeo K (2013) Basic concepts in physiologically based pharmacokinetic modeling in drug discovery and development. *CPT Pharmacometrics Syst Pharmacol* **2**:e63.Ke A, Barter Z, Rowland-Yeo K, and Almond L (2016) Towards a best practice approach in PBPK modeling: case example of developing a unified efavirenz model accounting for induction of CYPs 3A4 and 2B6. *CPT Pharmacometrics Syst Pharmacol* **5**:367–376.

Koziolek M, Schneider F, Grimm M, Modeβ C, Seekamp A, Roustom T, Siegmund W, and Weitschies W (2015) Intragastric pH and pressure profiles after intake of the high-caloric, high-fat meal as used for food effect studies. *J Control Release* **220** (Pt A):71–78.

Lavé T, Parrott N, Grimm HP, Fleury A, and Reddy M (2007) Challenges and opportunities with modelling and simulation in drug discovery and drug development. *Xenobiotica* **37**:1295–1310.

Li M, Zhao P, Pan Y, and Wagner C (2018) Predictive performance of physiologically based pharmacokinetic models for the effect of food on oral drug absorption: current status. *CPT Pharmacometrics Syst Pharmacol* **7**:82–89.

Lin L and Wong H (2017) Predicting oral drug absorption: mini review on physiologically-based pharmacokinetic models. *Pharmaceutics* **9**:41 DOI: doi: 10.3390/pharmaceutics9040041.

Mouly S, Lown KS, Kornhauser D, Joseph JL, Fiske WD, Benedek IH, and Watkins PB (2002) Hepatic but not intestinal CYP3A4 displays dose-dependent induction by efavirenz in humans. *Clin Pharmacol Ther* **72**:1–9.

Mouly S and Paine MF (2003) P-glycoprotein increases from proximal to distal regions of human small intestine. *Pharm Res* **20**:1595–1599.

Nestorov I (2007) Whole-body physiologically based pharmacokinetic models. *Expert Opin Drug Metab Toxicol* **3**:235–249.

Novi C, Bissoli F, Simonati V, Volpini T, Baroli A, and Vignati G (1980) Rifampin and digoxin: possible drug interaction in a dialysis patient. *JAMA* **244**:2521–2522.

Ono C, Hsyu PH, Abbas R, Loi CM, and Yamazaki S (2017) Application of physiologically based pharmacokinetic modeling to the understanding of bosutinib pharmacokinetics: prediction of drug-drug and drug-disease interactions. *Drug Metab Dispos* **45**:390–398.

Oswald S, Meyer zu Schwabedissen HE, Nassif A, Modess C, Desta Z, Ogburn ET, Mostertz J, Keiser M, Jia J, Hubeny A, et al. (2012) Impact of efavirenz on intestinal metabolism and transport: insights from an interaction study with ezetimibe in healthy volunteers. *Clin Pharmacol Ther* **91**:506–513.

Prueksaritanont T, Chu X, Gibson C, Cui D, Yee KL, Ballard J, Cabalu T, and Hochman J (2013) Drug-drug interaction studies: regulatory guidance and an industry perspective. *AAPS J* **15**:629–645.

Rautio J, Humphreys JE, Webster LO, Balakrishnan A, Keogh JP, Kunta JR, Serabjit-Singh CJ, and Polli JW (2006) In vitro p-glycoprotein inhibition assays for assessment of clinical drug interaction potential of new drug candidates: a recommendation for probe substrates. *Drug Metab Dispos* **34**:786–792.

Rodgers T, Leahy D, and Rowland M (2005) Physiologically based pharmacokinetic modeling 1: predicting the tissue distribution of moderate-to-strong bases. *J Pharm Sci* **94**:1259–1276.

Rostami-Hodjegan A and Tucker G (2004) 'In silico' simulations to assess the 'in vivo' consequences of 'in vitro' metabolic drug-drug interactions. *Drug Discov Today Technol* **1**:441–448.

Rowland M, Peck C, and Tucker G (2011) Physiologically-based pharmacokinetics in drug development and regulatory science. *Annu Rev Pharmacol Toxicol* **51**:45–73.

Sager JE, Yu J, Ragueneau-Majlessi I, and Isoherranen N (2015) Physiologically based pharmacokinetic (PBPK) modeling and simulation approaches: a systematic review of published models, applications, and model verification. *Drug Metab Dispos* **43**:1823–1837.

Shardlow CE, Generaux GT, Patel AH, Tai G, Tran T, and Bloomer JC (2013) Impact of physiologically based pharmacokinetic modeling and simulation in drug development. *Drug Metab Dispos* **41**:1994–2003.

Shebley M, Sandhu P, Emami Riedmaier A, Jamei M, Narayanan R, Patel A, Peters SA, Reddy VP, Zheng M, de Zwart L, et al. (2018) Physiologically based pharmacokinetic model qualification and reporting procedures for regulatory submissions: a consortium perspective. *Clin Pharmacol Ther* DOI: 10.1002/cpt.1013 [published ahead of print].

Shepard T, Scott G, Cole S, Nordmark A, and Bouzom F (2015) Physiologically based models in regulatory submissions: output from the ABPI/MHRA forum on physiologically based modeling and simulation. *CPT Pharmacometrics Syst Pharmacol* **4**:221–225.

Sjögren E, Westergren J, Grant I, Hanisch G, Lindfors L, Lennernäs H, Abrahamsson B, and Tannergren C (2013) In silico predictions of gastrointestinal drug absorption in pharmaceutical product development: application of the mechanistic absorption model GI-Sim. *Eur J Pharm Sci* **49**:679–698.

Syed YY, McCormack PL, and Plosker GL (2014) Bosutinib: a review of its use in patients with Philadelphia chromosome-positive chronic myelogenous leukemia. *BioDrugs* **28**:107–120.

Tachibana T, Kitamura S, Kato M, Mitsui T, Shirasaka Y, Yamashita S, and Sugiyama Y (2010) Model analysis of the concentration-dependent permeability of P-gp substrates. *Pharm Res* **27**:442–446.

Varma MV, Gardner I, Steyn SJ, Nkansah P, Rotter CJ, Whitney-Pickett C, Zhang H, Di L, Cram M, Fenner KS, et al. (2012) pH-Dependent solubility and permeability criteria for provisional biopharmaceutics classification (BCS and BDDCS) in early drug discovery. *Mol Pharm* **9**:1199–1212.

Vermeer LM, Isringhausen CD, Ogilvie BW, and Buckley DB (2016) Evaluation of ketoconazole and its alternative clinical CYP3A4/5 inhibitors as inhibitors of drug transporters: the in vitro effects of ketoconazole, ritonavir, clarithromycin, and itraconazole on 13 clinically-relevant drug transporters. *Drug Metab Dispos* **44**:453–459.

Wagner C, Pan Y, Hsu V, Grillo JA, Zhang L, Reynolds KS, Sinha V, and Zhao P (2015) Predicting the effect of cytochrome P450 inhibitors on substrate drugs: analysis of physiologically based pharmacokinetic modeling submissions to the US Food and Drug Administration. *Clin Pharmacokinet* **54**:117–127.

Wagner C, Pan Y, Hsu V, Sinha V, and Zhao P (2016) Predicting the effect of CYP3A inducers on the pharmacokinetics of substrate drugs using physiologically based pharmacokinetic (PBPK) modeling: an analysis of PBPK submissions to the US FDA. *Clin Pharmacokinet* **55**:475–483.

Williamson B, Dooley KE, Zhang Y, Back DJ, and Owen A (2013) Induction of influx and efflux transporters and cytochrome P450 3A4 in primary human hepatocytes by rifampin, rifabutin, and rifapentine. *Antimicrob Agents Chemother* **57**:6366–6369.

Zhang H, Xia B, Sheng J, Heimbach T, Lin TH, He H, Wang Y, Novick S, and Comfort A (2014) Application of physiologically based absorption modeling to formulation development of a low solubility, low permeability weak base: mechanistic investigation of food effect. *AAPS PharmSciTech* **15**:400–406.

Zhao P, Rowland M, and Huang SM (2012) Best practice in the use of physiologically based pharmacokinetic modeling and simulation to address clinical pharmacology regulatory questions. *Clin Pharmacol Ther* **92**:17–20.

Address correspondence to: Dr. Shinji Yamazaki, Pharmacokinetics, Dynamics and Metabolism, La Jolla Laboratories, Pfizer Worldwide Research and Development, 10777 Science Center Drive, San Diego, CA 92121. E-mail: shinji.yamazaki@pfizer.com